M-2522

J. Chem. Thermodynamics **1990**, 22, 1035–1057

Thermodynamics of copper sulfides

IV. Heat capacity and thermodynamic properties of $Cu_{1.90}S$ from 5 K to 750 K, $Cu_{1.95}S$ from 5 K to 1000 K, $Cu_{1.98}S$ from 300 K to 1000 K, and $Cu_{1.995}S$ from 300 K to 750 K [a]

SVEIN STØLEN, FREDRIK GRØNVOLD,

Department of Chemistry, University of Oslo, Blindern, 0315 Oslo 3, Norway

and EDGAR F. WESTRUM, JR.

Department of Chemistry, University of Michigan, Ann Arbor, MI 48109, U.S.A.

(Received 5 June 1990)

The heat capacities of $Cu_{1.90}S$, $Cu_{1.95}S$, $Cu_{1.98}S$, and $Cu_{1.995}S$ have been measured by adiabatic-shield calorimetry. All samples have been characterized by powder X-ray diffraction in the temperature interval studied. A revised version of the copper-rich part of the phase diagram is presented. All transitions are characterized by hysteresis in the attainment of equilibrium and a greater or lesser dependence on thermal history and/or thermal recycling. Thermodynamic functions have been evaluated and selected values are, for $R = 8.3144\ J \cdot K^{-1} \cdot mol^{-1}$:

	$C_{p,m}/R$	$\Delta_0^T S_m/R$	Φ_m°/R	T/K
(1/2.90)$Cu_{1.90}S$	(3.166)	4.654	2.5148	298.15
	3.478	8.080	4.9280	700
(1/2.92)$Cu_{1.95}S$	3.109	4.679	2.5353	298.15
	3.446	8.145	4.9391	700
	3.420	9.361	6.0945	1000
	$C_{p,m}/R$	$\Delta_{298.15\,K}^T S_m^\circ/R$	$\Delta_{298.15\,K}^T H_m^\circ/(R \cdot K)$	T/K
(1/2.98)$Cu_{1.98}S$	3.042	0	0	298.15
	3.395	3.529	1643.4	700
	3.384	4.723	2646.9	1000
(1/2.995)$Cu_{1.995}S$	3.027	0	0	298.15
	(4.02)	3.564	1660.7	700

1. Introduction

Despite extensive research on (copper + sulfur), the phase relations in the region from Cu_2S to $Cu_{1.90}S$ are still not well established. In addition to uncertainties as to

[a] The preceding papers in this series are cited in references 1 to 3.

0021-9614/90/111035+23 $02.00/0

the extension of the homogeneity ranges of the stable phases, djurleite and chalcocite, ambiguity is created by metastable phases. The present paper concerns primarily the heat capacities and thermodynamic properties of $Cu_{1.90}S$, $Cu_{1.95}S$, $Cu_{1.98}S$, and $Cu_{1.995}S$. However, during the course of this study a large number of "anomalies" were observed in the heat capacities, and a structural study was made to characterize the different transitions.

At room temperature three stable solid phases are found in the Cu_2S to $Cu_{1.75}S$ region. In addition to chalcocite (Cu_2S) and anilite ($Cu_{1.75}S$), which have been discussed in previous papers in this series,[1 3] the djurleite phase is also stable. This phase was discovered by Djurle[4] who reported the ratio $n(Cu)/n(S)$ to be 1.96. Subsequent studies differ regarding the compositional limits of djurleite.[4 11] Whereas Cook[8] claimed that the phase region is very narrow (1.93 ± 0.015), Luquet *et al.*[9] found a broad range of homogeneity (1.92 to 1.96). It is generally agreed that djurleite decomposes into high chalcocite and high digenite around 366 K. The structure of djurleite was first described as orthorhombic by Takeda *et al.*[6] Later refinements from natural specimens revealed, however, a slight monoclinic distortion (space group $P2_1/n$).[12 14] According to these refinements, the unit cell contains eight $Cu_{31}S_{16}$ units, giving a ratio $n(Cu)/n(S)$ of 1.938. This is in agreement with the sulfur-rich phase limit reported.[8 11] The copper-rich phase boundary is generally assumed to be around 1.96 to 1.97,[4 11] which might indicate that the djurleite field is restricted by ratios $n(Cu)/n(S)$ of 62/32 and 63/32 (1.938 to 1.969).[14] The assumption of a homogeneity range necessarily implies partly occupied sites which give rise to positional disorder in the intermediate range.

In addition to these stable phases, the existence of numerous metastable phases has been reported.[5, 10, 15 19] One of the main complications during the present study was the occurrence of a phase with tetragonal structure in the region $Cu_{1.95}S$ to $Cu_{1.98}S$. This phase, also first reported by Djurle,[4] was claimed to be metastable at low pressures by Roseboom.[5] More recently, Skinner[18] confirmed that the tetragonal phase is a high-pressure polymorph of chalcocite with invariance point at 380 K and 80 MPa. In an electrochemical study Potter[11] found that the phase was unstable by about 1 $kJ \cdot mol^{-1}$ in the range 388 K to 418 K with respect to stable (high chalcocite + high digenite). The transition of this metastable phase into djurleite is extremely sluggish. Roseboom[5] reported the equilibration time at room temperature to be 18 months for a sample consisting of (2/3) tetragonal phase and (1/3) djurleite, which had been slowly cooled from 530 K.[5] The tetragonal structure has been described in some detail by Janosi.[15] According to Kazinets *et al.*[20] the tetragonal structure may be considered as a superstructure of high digenite with $c = 2a_{fcc}$.

Another metastable phase, protodjurleite, was obtained by Mulder[19] by cooling samples with $n(Cu)/n(S)$ between 1.96 and 1.99. His findings were confirmed by Potter.[11] A hexagonal polymorph of digenite was observed by Cook *et al.*,[17] while Eliseev *et al.*[16] and Mathieu and Rickert[10] reported the existence of a phase with $n(Cu)/n(S) \approx 1.90$. It was remarked by Potter,[11] however, that the latter observations were based on an incorrect interpretation of the data.

No earlier heat capacities exist for the five compositions studied here. For the

related compositions $Cu_{1.998}S$, $Cu_{1.988}S$, and $Cu_{1.9535}S$ heat capacities in the range 170 K to 800 K have been reported by Kubaschewski[21] in diagrammatic form. Some information about the phase relations in the copper-rich region of (copper + sulfur) have also been obtained by Luquet *et al.*[9] by d.t.a.

2. Experimental

The copper sulfides were prepared directly from the elements. The copper was in the form of a continuous rod, >99.999 mass per cent pure, from the American Smelting and Refining Co., New Jersey. The sulfur was 99.9999 mass per cent pure crystals from Koch-Light Laboratories, Colnbrook, England. The mixture of the elements was heated in an evacuated and sealed vitreous silica tube, constricted at the middle by a smaller-diameter tube. Copper was placed in one part of the tube and sulfur in the other, and the tube was put into a slightly inclined tube furnace with the sulfur-containing compartment protruding. The copper was heated to 620 K and the sulfur was allowed to melt and flow into the hotter part of the tube. When most of the sulfur had combined with the copper, a heating pad wound around the exterior end of the silica tube was used to bring the remaining sulfur into reaction overnight. The empty half of the silica tube was sealed off and discarded before tempering the sample at 670 K for 24 h. The sample was then finally crushed and transferred to the calorimetric ampoule.

The characterization of the samples was done by powder X-ray diffraction as described in reference 3. The room temperature X-ray powder photographs were, however, taken in Guinier-Hägg cameras of 50 mm diameter with Cr $K\alpha_1$ radiation, ($\lambda = 228.962$ pm). This was done in order to obtain better resolution of the diffraction lines. The phases observed in the three samples, as well as their lattice constants, are presented in table 1 together with results by previous investigators. The d.t.a. method has been described elsewhere.[3]

The calorimetry previously described,[1] includes the low-temperature (5 K to 350 K) work done at the University of Michigan[24] and the high-temperature work (300 K to 1000 K) at the University of Oslo.[25] The heat capacity of the samples represented from about 95 per cent to 80 per cent of the total in the low-temperature calorimeter and about 50 per cent in the high-temperature calorimeter outside the transition regions.

3. Results and discussion

STRUCTURAL CHARACTERIZATION AND PHASE RELATIONS

Despite numerous studies concerning the very complex phase relations below 400 K in the $Cu_{1.75}S$ to Cu_2S region of (copper + sulfur), no consensus about the extension and/or stability of the intermediate phases has been reached. Hence, further structural characterizations of the calorimetric samples were needed.

At room temperature anilite, djurleite, and low chalcocite are observed in the X-ray powder photographs of thoroughly annealed samples. Results and calculations

TABLE 1. Phases characterized by X-ray powder diffraction at room temperature. The djurleite structure is indexed according to an orthorhombic cell. Small and varying amounts of a phase with tetragonal structure were observed in $Cu_{1.95}S$ and $Cu_{1.98}S$

x in Cu_xS	Phase	Unit-cell dimensions a/pm	b/pm	c/pm	β/π	Reference
1.90	Djurleite	2691.9 ± 1.5	1573.8 ± 0.7	1358.0 ± 0.6		present
	Anilite	five strongest lines				
1.95	Djurleite	2691.1 ± 1.1	1575.8 ± 0.6	1357.2 ± 0.4		present
1.98	Djurleite	2692.2 ± 1.3	1576.4 ± 0.8	1355.8 ± 0.8		present
	L-Chalcocite	1524.4 ± 0.4	1189.2 ± 0.2	1351.6 ± 0.3	2.0300 ± 0.0002	
1.995	Djurleite	some of the strongest lines				present
	L-Chalcocite	1523.6 ± 0.4	1189.5 ± 0.2	1350.5 ± 0.3	2.0300 ± 0.0002	
2.00	L-Chalcocite	1524.7 ± 0.4	1189.1 ± 0.3	1349.0 ± 0.4	2.0310 ± 0.0003	14
2.00	L-Chalcocite	1524.6 ± 0.4	1188.4 ± 0.2	1349.4 ± 0.3	2.0307 ± 0.0002	22
2.00	L-Chalcocite	1523.5 ± 0.3	1188.5 ± 0.2	1349.6 ± 0.2	2.0291 ± 0.0002	23
1.934	Djurleite	2689.6 ± 0.6	1569.4 ± 0.3	1353.6 ± 0.3		23
1.96	Djurleite	2686 ± 2	1570.0 ± 0.6	1352.8 ± 0.6		4
1.97	Djurleite	2692 ± 5	1571 ± 3	1356 ± 3		6
1.94	Djurleite	2689.7 ± 0.7	1574.5 ± 0.3	1356.5 ± 0.5	1.5731 ± 0.0003	13, 14

for anilite are given in reference 3, whereas corresponding results for djurleite (in $Cu_{1.95}S$) and low chalcocite (in Cu_2S) are presented here in table 2. The calculated intensities are based on the structural quantities given in reference 14. The obtained unit-cell dimensions, given in table 1, are in good accord with previously published values. The slight scatter in the cell dimensions is related mainly to difficulties in resolution of diffraction lines when two phases with large unit cells are present. In $Cu_{1.95}S$ and $Cu_{1.98}S$ the earlier-reported phase with tetragonal structure is present to some extent. According to Potter[11] this phase becomes unstable in the temperature range 388 K to 418 K. However, no low-temperature X-ray studies have been made so far in this composition region. Thus, the transition near 220 K in $Cu_{1.95}S$, observed in the present heat-capacity study, and also by d.t.a. of $Cu_{1.98}S$ here, and of $Cu_{1.9535}S$ by Kubaschewski,[21] is of so far unknown origin. X-ray powder photographs of $Cu_{1.95}S$ show that the djurleite phase remains unchanged around 220 K. Five reflections which are present at low temperatures, and apparently do not belong to low chalcocite, or djurleite, disappear around 220 K. Furthermore, seven new reflections which may be indexed in terms of a tetragonal cell with $a = (400.78 \pm 0.14)$ pm and $c = (1125.8 \pm 0.9)$ pm occur above the transition temperature. The transition appears to be of first order, showing temperature hysteresis ($T_h = 238$ K and $T_c = 224$ K, as detected by d.t.a.).

The structure and stoichiometry of the low-temperature phase are not yet known. Taking the very low transition temperature into consideration, the low-temperature phase and the tetragonal phase most probably have the same stoichiometry. Both low-temperature phases are observed only in the range $Cu_{1.95}S$ to $Cu_{1.99}S$, hence indicating stoichiometries around $Cu_{1.96\text{ to }1.97}S$. The position of the reflections observed at the lowest temperatures as well as the tetragonal reflections are given in table 2. The five low-temperature reflections listed in the table all disappear at higher

TABLE 2. X-ray powder results for synthetic djurleite ($Cu_{1.95}S$) and synthetic low chalcocite (Cu_2S) at 295 K with Cr $K\alpha_1$ radiation, and for the most characteristic reflections of the low-temperature phase and the tetragonal phase in $Cu_{1.95}S$ (obtained with Cu $K\alpha_1$ radiation, but multiplied by the factor 2.2090 for direct comparison with the djurleite results)

I_{obs}	hkl	$10^5(\sin\theta)^2$	I_{calc}	I_{obs}	hkl	$10^5(\sin\theta)^2$	I_{calc}
			Cu_2S — low chalcocite				
vw	111/$\bar{2}$11	3199	51	m	042/$\bar{2}$42	18449	192
vw	022/$\bar{2}$22	7249	45	w	114/$\bar{3}$14	18739	55
w	221/$\bar{3}$21	8788	54	s	$\bar{3}$15	19109	126
vw	202/$\bar{4}$02	9151	16	m	241/$\bar{3}$41	19963	89
s	122/$\bar{3}$22	9384	229	s	402/$\bar{6}$02	20514	197
m	212/$\bar{4}$12	10124	156	vs	412/$\bar{6}$12	21397	341
m	032/$\bar{2}$32	11913	170	vs	204/$\bar{6}$04	22766	541
s	$\bar{1}$04/$\bar{3}$04	12214	229	s	$\bar{1}$52	26112	130
s	222/$\bar{4}$22	12921	162	s	$\bar{3}$16	26875	295
s	$\bar{3}$14/$\bar{1}$14	13138	237	w	$\bar{4}$44/044	29107	108
m	132/$\bar{3}$32	14027	127	w	$\bar{1}$26/$\bar{5}$26	32346	65
s	312/$\bar{5}$12	15056	297	vs	060	33339	383
w	014/$\bar{4}$14	15236	89	vs	630	33662	1000
vw	$\bar{1}$24/$\bar{3}$24	15974	46	m	$\bar{7}$21	34090	66
m	$\bar{1}$41/041	17141	123	s	450	34396	189
vs	240	17644	317	m	026/$\bar{6}$26	35933	81
vw	024/$\bar{4}$24	17999	23	m	532/$\bar{7}$32	36494	107
			$Cu_{1.95}S$ — djurleite				
vw	331	7083	42	w	343	16516	44
vw	611	7748	8	vw	451	16814	26
vw	313/$\bar{3}$13	8574	59	vw	604	17828	47
m	332/$\bar{3}$32	9205	119	w	115	18483	84
vw	413	9779	24	vw	305	19383	10
w	323/323/711	10133	85	w	153	19764	72
m	440	11339	201	w	315/$\bar{3}$15	19995	84
w	800	11575	63	w	415/353	21184	78
vw	721	11696	27	w	162	22023	38
vw	233/$\bar{2}$33	11857	34	m	1.1.10	22414	89
w	114/$\bar{1}$14	12104	34	s	804/$\bar{8}$04	22899	320
w	333/$\bar{3}$33	12810	121	s	1.1.11	23134	103
w	314/$\bar{3}$14	13493	106	w	216/$\bar{2}$16	26872	56
m	151/433	14079	90	w	753	28527	31
w	821/802	14379	115	w	326	29342	33
w	414	14838	61	w	570	30395	90
w	143	15009	42	w	1.3.10/571	31123	66
m	351/$\bar{3}$51	15483	103	vs	080	33743	450
m	533	15577	85	vs	046	34131	1000
m	911	15846	118				
			$Cu_{1.95}S$ — tetragonal $T \approx 250$ K				
w	102	12260		m	113	25602	
m	110	16271		s	114	32277	
vs	111	17347		w	202	36679	
vs	104	24700		w	211	41820	
			$Cu_{1.95}S$ — low-temperature phase $T \approx 150$ K				
s		21811		w		39026	
s		24050		vw		43397	
w		31584					

TABLE 3. Phases occurring in $Cu_{1.90}S$, $Cu_{1.95}S$, $Cu_{1.98}S$, $Cu_{1.99}S$, and $Cu_{1.995}S$ in the range 293 K to 525 K

T / K	x in Cu_xS				
	1.90	1.95	1.98	1.99	1.995
293	Dj + An	Dj	Dj + LoCh	Dj + LoCh	Dj + LoCh
325	Dj + LoDg	Dj	Dj + LoCh	Dj + LoCh	Dj + LoCh
355	Dj + HiDg	Dj	Dj + LoCh	Dj + LoCh	Dj + LoCh
390	HiDg + HiCh	HiDg + HiCh	HiDg + HiCh	HiCh	HiCh
425	HiDg + HiCh	HiDg + HiCh	HiDg + HiCh	HiDg + HiCh	HiDg + HiCh
525	HiDg	HiDg + HiCh	HiDg + HiCh	HiDg + HiCh	HiDg + HiCh

temperatures. The low-temperature structure may, however, be characterized by additional reflections present also at higher temperatures.

At room temperature X-ray photographs of $Cu_{1.98}S$ and $Cu_{1.995}S$ show the presence of both low chalcocite and djurleite as well as the tetragonal phase. Thus, one of these phases, most probably the tetragonal one, is metastable at this temperature. The relative proportions of the phases depend on the previous thermal history as the transition of the tetragonal phase to the stable assemblage is extremely slow. In addition, phase separation might originate from insufficient thermal equilibration during cooling. This aspect causes variability in the heat capacities in the transitional region for the different measurement series, which will be further discussed below.

The results of the X-ray-diffraction-based phase analysis in the range 293 K to 525 K are summarized in table 3. In addition, the tetragonal phase is observed in varying amounts in $Cu_{1.95}S$, $Cu_{1.98}S$, and $Cu_{1.995}S$ at 390 K and below. Although the presently studied samples are well characterized as a function of temperature, the extensions of the djurleite- and high-chalcocite fields have not been properly delineated. The djurleite transition is observed alone in $Cu_{1.90}S$ and $Cu_{1.95}S$. In $Cu_{1.98}S$ and $Cu_{1.995}S$ eutectoid formation of high chalcocite from (djurleite + low chalcocite) is observed, and also the low- to high-chalcocite transition.

A new phase diagram for the copper-rich part of (copper + sulfur) is presented in figure 1. It is based in part on the new structural and heat-capacity results obtained here which indicate that high chalcocite is formed eutectoidally from djurleite and low chalcocite at 366.2 K, and that its composition is approximately $Cu_{1.97}S$. The djurleite phase is taken to exist over the composition range $Cu_{1.938}S$ to $Cu_{1.969}S$ as reported by Potter,[11] whereas the extension of the homogeneity range of high chalcocite is chosen in consistency with the presently reported X-ray and heat-capacity results.

HEAT CAPACITIES

The experimental heat capacities for $(1/2.90)Cu_{1.90}S$, $(1/2.95)Cu_{1.95}S$, $(1/2.98)Cu_{1.98}S$, and $(1/2.995)Cu_{1.995}S$ from both low- and high-temperature ranges, are listed in chronological order in table 4 for the mean temperatures. The

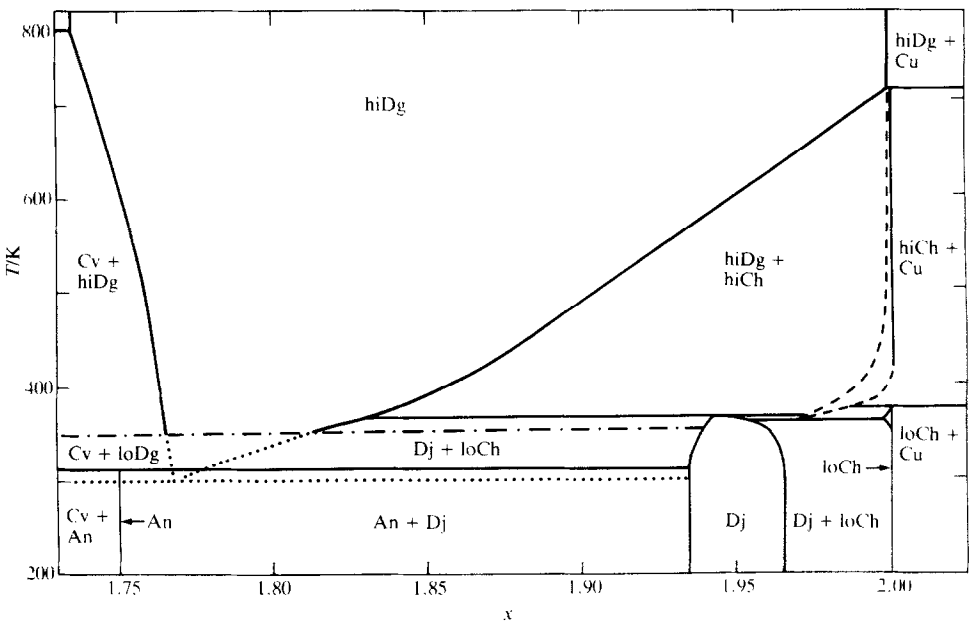

FIGURE 1. Part of the (copper + sulfur) phase diagram. Cv, covellite, CuS; An, anilite, $Cu_{1.75}S$; loDg, low digenite, $Cu_{2-x}S$ with $0.18 < x < 0.23$; hiDg, high digenite, $Cu_{2-x}S$ with $0 < x < 0.27$; Dj, djurleite, $Cu_{62}S_{32}$ to $Cu_{63}S_{32}$; loCh, low chalcocite, Cu_2S; hiCh, high chalcocite, $Cu_{2-x}S$, $0 < x < 0.02$. ····, Presently assumed eutectoid decomposition lines for low digenite; —·—, low-digenite to high-digenite transition temperatures; — — —, presently assumed phase limits for high chalcocite.

approximate temperature increments used in the determinations can usually be inferred from the adjacent mean temperatures in table 4.

Twice the standard deviation in the measured low-temperature heat capacity is about 1 per cent from 8 K to 30 K, 0.1 per cent from 30 K to 300 K, and 0.2 per cent from 300 K to 350 K. In the higher-temperature region it is about 0.3 per cent. The smoothed heat capacities for $Cu_{1.95}S$ and $Cu_{1.98}S$ are in reasonable agreement with those reported by Kubaschewski[21] for $Cu_{1.9535}S$ and $Cu_{1.988}S$, respectively. The heat capacities reported by Kubaschewski were, however, presented only as a small figure, and a proper comparison with the present results is not possible.

TRANSITIONAL ENTHALPIES AND ENTROPIES

The enthalpies and entropies of the different transitions are given in table 5. Due to the presence of several partly overlapping heat-capacity contributions the values of the separate transitional increments depend considerably on the way the resolution is made. In addition, the background level chosen for evaluating the excess functions is of decisive importance in the comparison of the different transitions. It should also be noted that the transitional evaluations from series with small energy increments and long stabilization times are relatively more sensitive to temperature-drift corrections and therefore less accurate than those from series with larger energy

TABLE 4. Heat capacities of $(1/2.90)Cu_{1.90}S$, $(1/2.95)Cu_{1.95}S$, $(1/2.98)Cu_{1.98}S$, and $(1/2.995)Cu_{1.995}S$. ($R = 8.3144\ J \cdot K^{-1} \cdot mol^{-1}$)

T K	$C_{p,m}$ R	T K	$C_{p,m}$ R	T K	$C_{p,m}$ R	T K	$C_{p,m}$ R	T K	$C_{p,m}$ R	T K	$C_{p,m}$ R
					$M\{(1/2.90)Cu_{1.90}S\} = 52.691\ g \cdot mol^{-1}$						
					High-temperature measurements — University of Oslo						
Series I		394.84	4.722	506.92	3.430	633.94	3.453	Series II		366.59	16.081
303.28	3.280	403.03	4.675	517.28	3.428	644.81	3.455	346.11	3.922	367.72	7.823
313.18	3.382	411.20	4.804	527.69	3.421	655.73	3.459	348.36	3.999	369.50	4.420
322.92	3.495	419.64	4.306	538.14	3.418	666.71	3.457	351.37	4.174	371.64	4.317
332.48	3.630	428.65	3.939	548.63	3.427	677.73	3.465	354.32	4.368	373.80	4.300
341.82	3.826	437.97	3.916	559.15	3.437	688.79	3.469	356.43	4.493	375.96	4.300
350.80	4.193	447.40	3.846	569.69	3.442	699.90	3.470	358.53	4.456	378.13	4.307
358.99	5.222	456.95	3.796	580.27	3.446	711.06	3.477	360.60	4.730	380.29	4.321
364.68	13.675	466.60	3.737	590.88	3.451	722.25	3.481	362.32	5.162	382.44	4.401
370.21	5.500	476.41	3.631	601.55	3.446	733.51	3.481	363.96	8.343	384.57	4.486
378.16	4.347	486.43	3.510	612.30	3.440	744.81	3.481	365.09	14.697	386.67	4.602
386.60	4.568	496.61	3.465	623.10	3.440			365.85	20.567	388.74	4.683
					Low-temperature measurements — University of Michigan						
Series III		194.61	2.7316	244.14	2.9236	324.44	3.2913	Series X		30.22	0.6179
76.96	1.6452	199.77	2.7556	249.32	2.9425	329.53	3.3518	9.519	0.0429	31.67	0.6627
80.34	1.7100	204.93	2.7779	254.50	2.9620	Series VI		10.022	0.0495	33.20	0.7088
84.31	1.7716	210.11	2.7973	259.67	2.9813	276.02	3.0721	10.483	0.0565	34.81	0.7570
88.51	1.8336	220.45	2.8423	264.87	2.9993	306.08	3.2881	Series XI		36.50	0.8051
92.95	1.8936	225.61	2.8609	270.09	3.0205	324.24	3.2756	9.87	0.0475	38.28	0.8548
97.63	1.9522	230.78	2.8784	280.38	3.0672	329.53	3.3518	10.41	0.0558	40.15	0.9046
102.54	2.0133	235.95	2.8988	285.55	3.0992	Series VII		10.90	0.0638	42.11	0.9554
107.58	2.0721	246.30	2.9360	290.69	3.1640	100.26	1.9650	11.34	0.0734	44.17	1.0076
112.63	2.1291	251.47	2.9529	295.74	3.3162	137.23	2.3641	11.92	0.0833	46.34	1.0609
117.70	2.1818	256.64	2.9740	300.63	3.6482	175.97	2.6339	12.48	0.0948	48.62	1.1150
122.79	2.2349	Series IV		305.54	3.7971	Series VIII		13.05	0.1063	51.02	1.1690
127.88	2.2859	176.94	2.6411	310.98	3.2998	281.66	3.0943	13.65	0.1200	53.53	1.2234
132.97	2.3361	186.26	2.6826	316.55	3.2578	310.88	3.4724	14.28	0.1360	56.18	1.2780
138.06	2.3830	192.42	2.7158	321.72	3.2956	328.30	3.3639	14.93	0.1530	58.96	1.3365
143.17	2.4253	197.58	2.7389	326.84	3.3548	333.25	3.5044	15.62	0.1713	61.88	1.3943
148.28	2.4648	202.74	2.7627	331.93	3.4493	Series IX		19.25	0.2747	64.95	1.4489
153.40	2.5024	207.91	2.7824	336.93	3.5738	273.98	3.0303	22.93	0.3896	68.19	1.5099
158.55	2.5366	213.09	2.8030	341.66	3.9207	303.79	3.4120	23.91	0.4199	71.50	1.5654
163.69	2.5695	218.26	2.8226	346.13	4.2232	321.50	3.3008	25.05	0.4561	75.04	1.6246
168.83	2.6019	223.44	2.8451	Series V		326.60	3.3116	26.25	0.4937	78.79	1.6872
173.98	2.6297	228.64	2.8706	275.77	3.0641	331.65	3.3895	27.51	0.5334	82.72	1.7515
179.13	2.6554	233.79	2.8894	306.07	3.2319			28.83	0.5745	86.86	1.8155
184.29	2.6826	238.96	2.9087								
					High-temperature measurements — University of Oslo						
Series XII		327.39	3.439	358.95	5.174	369.02	5.246	399.67	4.643	524.09	3.413
261.50	2.964	331.62	3.535	360.59	5.708	370.71	4.228	410.79	4.354	537.49	3.399
270.80	3.009	335.67	3.685	362.13	6.545	372.30	4.338	422.37	4.046	550.96	3.387
279.99	3.069	339.77	3.927	363.50	7.903	Series XIII		434.31	3.919	564.50	3.410
289.13	3.120	343.64	4.366	364.64	11.161	341.76	3.700	446.51	3.840	578.08	3.411
295.83	3.245	347.36	4.493	365.52	15.563	353.57	4.364	458.91	3.731	591.70	3.412
300.14	3.534	350.97	4.759	366.16	21.192	362.56	9.802	471.54	3.680	605.31	3.430
304.28	3.656	353.67	4.576	366.71	22.816	369.13	9.759	484.38	3.524	618.91	3.434
308.63	3.418	355.47	4.756	367.22	26.256	377.99	4.502	497.48	3.423	632.69	3.463
318.80	3.273	357.23	4.938	367.80	15.082	388.87	4.793	510.74	3.383	646.38	3.466
323.12	3.360										

TABLE 4—*continued*

T K	$C_{p,m}/R$	T K	$C_{p,m}/R$	T K	$C_{p,m}/R$	T K	$C_{p,m}/R$	T K	$C_{p,m}/R$	T K	$C_{p,m}/R$
$M\{(1/2.95)Cu_{1.95}S\} = 52.875\ g \cdot mol^{-1}$											
High-temperature measurements — University of Oslo											
Series I		494.85	3.822	705.62	3.424	422.84	4.661	375.10	4.521	789.61	3.419
322.95	3.246	505.57	3.825	718.06	3.430	432.51	4.163	379.78	4.507	801.28	3.425
333.93	3.324	516.32	3.833	730.67	3.439	442.78	3.804	384.45	4.560	813.00	3.406
344.72	3.482	527.11	3.828	743.32	3.435	453.28	3.851	389.10	4.617	826.86	3.392
354.87	4.279	537.94	3.840	756.06	3.421	463.75	3.880	393.72	4.676	838.76	3.404
362.29	10.798	548.78	3.872	768.90	3.430	474.27	3.864	398.24	4.977	850.68	3.401
368.26	7.621	559.63	3.904	Series II		484.86	3.850	402.50	5.358	862.63	3.392
376.27	4.600	570.48	3.940	313.06	3.201	495.54	3.822	406.83	4.858	881.41	3.389
385.54	4.645	581.31	3.981	324.06	3.271	506.28	3.803	411.39	4.762	899.56	3.400
394.77	4.718	592.08	4.103	334.95	3.341	517.08	3.801	415.98	4.738	911.56	3.380
403.85	4.983	603.34	3.660	345.68	3.495	527.97	3.805	420.59	4.752	924.05	3.370
412.93	4.762	614.88	3.441	355.80	4.249	Series III		425.20	4.762	936.40	3.376
422.16	4.781	626.75	3.423	362.73	13.964	347.96	3.495	429.81	4.777	948.82	3.398
431.76	4.211	638.67	3.423	368.61	6.289	353.18	3.768	434.45	4.704	961.27	3.410
442.00	3.828	645.02	3.413	377.13	4.422	358.04	4.597	439.26	4.201	973.74	3.399
452.51	3.860	657.03	3.421	386.54	4.505	361.75	9.646	444.37	3.795	986.27	3.401
463.02	3.858	669.09	3.415	395.80	4.779	364.12	15.984	Series IV		998.88	3.429
473.58	3.851	681.22	3.429	404.53	5.150	366.60	8.637	770.78	3.431		
484.19	3.832	693.38	3.427	413.54	4.724	370.45	4.564	779.43	3.407		
Low-temperature measurements — University of Michigan											
Series V		196.42	2.7535	337.78	3.3086	Series XIII		221.51	3.1773	5.61	0.0074
204.79	2.7956	206.43	2.8029	345.83	3.3859	201.24	2.7740	221.88	3.1757	6.70	0.0133
212.69	2.8262	Series VIII		Series XI		205.54	2.7902	222.25	3.1445	7.63	0.0192
222.46	2.8590	200.14	2.7699	206.81	2.7978	209.82	2.8048	222.62	3.1650	8.37	0.0285
238.18	2.9122	209.45	2.8121	210.84	2.8196	214.07	2.8231	223.18	3.1075	9.36	0.0411
Series VI		218.81	3.2850	213.85	2.8417	217.25	2.8407	224.13	3.0653	10.31	0.0579
214.10	2.8649	228.37	3.0374	215.83	2.8793	218.72	2.8469	227.40	2.9581	11.24	0.0722
222.97	2.8629	238.64	2.9291	217.67	2.9154	219.55	2.8498	232.80	2.9141	12.26	0.0922
233.51	2.8893	248.29	2.9426	218.27	3.0353	220.17	2.8544	Series XV		13.43	0.1186
246.34	2.9311	257.14	2.9664	219.21	3.0741	220.59	2.8553	213.43	2.8276	14.74	0.1529
252.30	2.9495	265.76	2.9953	220.13	3.2611	221.00	2.8613	218.18	2.8911	16.24	0.1908
260.04	2.9787	275.09	3.0270	220.96	3.8485	221.41	2.8752	220.65	2.9742	19.96	0.3016
270.55	3.0160	285.18	3.0630	221.76	3.6225	221.82	2.8943	221.62	3.0165	22.35	0.3759
284.29	3.0634	295.01	3.0976	222.59	3.4725	222.23	2.8798	222.58	3.0442	25.27	0.4694
299.18	3.1139	Series IX		223.48	3.2815	222.64	2.8995	223.53	3.0459	28.21	0.5622
Series VII		117.91	2.1976	224.41	3.0913	223.25	2.8926	224.48	3.0215	30.90	0.6489
90.48	1.8770	125.69	2.2758	225.83	3.0053	224.69	2.8864	227.38	2.9683	34.34	0.7527
99.18	1.9870	134.23	2.3558	228.73	2.9443	Series XIV		Series XVI		37.82	0.8525
107.81	2.0878	143.55	2.4338	Series XII		203.20	2.7799	54.94	1.2662	41.54	0.9526
117.11	2.1933	152.59	2.5029	215.21	2.8554	206.83	2.7948	60.38	1.3776	45.59	1.0550
127.08	2.2925	161.52	2.5623	217.69	2.9069	211.01	2.8160	66.96	1.5020	50.01	1.1599
136.89	2.3796	170.75	2.6212	219.29	3.0440	213.95	2.8303	74.37	1.6256	54.76	1.2626
146.80	2.4613	Series X		220.86	3.2165	215.63	2.8512	82.63	1.7606	Series XVIII	
156.78	2.5338	213.79	2.8981	222.53	3.2750	217.67	2.9154	91.09	1.8832	93.08	1.3115
166.64	2.5989	273.78	3.0250	224.27	3.1614	219.28	3.0162	100.87	2.0054	167.32	2.5960
176.48	2.6558	306.60	3.1417	226.69	3.0304	220.07	3.0648	111.92	2.1328	204.52	2.7831
186.43	2.7055	317.12	3.1882	232.29	2.9535	220.67	3.1491	Series XVII		210.63	2.8107
		327.53	3.2420			221.10	3.1635	4.55	0.0035		

TABLE 4 - *continued*

T K	$C_{p,m}$ R	T K	$C_{p,m}$ R	T K	$C_{p,m}$ R	T K	$C_{p,m}$ R	T K	$C_{p,m}$ R	T K	$C_{p,m}$ R
High-temperature measurements — University of Oslo											
Series XIX		Series XX		372.99	4.659	362.39	19.364	369.70	4.799	402.99	4.723
300.13	3.089	351.10	3.564	375.68	4.561	362.77	20.314	370.73	4.791	406.19	4.590
309.94	3.140	354.09	3.908	Series XXI		363.14	20.158	371.78	4.607	409.40	4.542
319.64	3.216	356.89	4.604	342.62	3.363	363.50	22.130	372.82	4.706	412.65	4.460
329.24	3.268	359.32	6.360	346.40	3.419	363.87	20.098	374.89	4.813	415.95	4.251
338.75	3.352	361.18	10.573	350.12	3.661	364.27	17.524	377.97	4.815	419.32	4.162
348.12	3.476	362.50	15.972	353.75	3.766	364.70	16.778	381.08	4.721	422.72	4.159
356.72	4.635	363.50	20.446	357.16	4.614	365.14	15.527	384.21	4.752	426.15	4.089
362.17	18.354	364.51	15.503	359.27	5.655	365.63	13.507	387.34	4.724	429.60	4.077
365.29	16.044	365.89	9.817	360.16	7.164	366.20	11.081	390.46	4.812	433.06	4.040
370.65	5.250	367.88	5.622	360.90	9.585	366.85	8.857	393.57	4.839	436.55	3.994
378.24	4.766	370.36	4.717	361.51	13.098	367.68	5.926	396.69	4.752	440.05	3.981
386.09	4.759			361.98	16.850	368.67	4.995	399.87	4.781		
$M\{(1/2.98)Cu_{1.98}S\} = 52.982\ g \cdot mol^{-1}$											
High-temperature measurements — University of Oslo											
Series I		364.91	10.484	575.61	3.777	955.04	3.329	371.35	12.587	379.19	3.868
313.52	3.158	366.46	39.474	585.86	3.816	966.70	3.330	371.75	13.526	380.25	3.905
326.57	3.199	368.16	8.494	596.16	3.825	978.41	3.348	372.11	14.809	381.31	3.955
336.71	3.261	370.61	11.531	606.48	3.821	990.16	3.365	372.46	15.180	Series VII	
346.77	3.322	372.54	13.920	616.79	3.887	1001.97	3.382	372.79	16.133	361.20	3.346
356.64	3.519	374.78	7.802	627.11	3.973	Series V		373.09	16.456	363.40	3.530
363.89	10.103	378.70	3.956	637.41	3.955	297.97	3.055	373.36	23.972	365.19	7.048
368.48	11.235	383.32	3.988	647.62	4.008	303.80	3.073	373.70	12.196	366.01	51.542
372.77	11.753	387.90	4.033	657.79	4.044	309.65	3.090	374.14	13.378	366.19	141.04
379.13	4.633	392.42	4.100	668.13	3.890	315.47	3.098	374.81	4.894	366.42	35.553
387.96	4.077	396.86	4.223	678.98	3.573	321.23	3.156	375.78	3.893	367.20	8.488
396.92	4.296	401.25	4.365	690.10	3.440	325.54	3.148	376.83	3.874	368.40	8.868
405.61	4.505	405.57	4.486	701.42	3.391	328.40	3.180	377.88	3.991	369.52	10.327
414.11	4.575	409.84	4.534	712.80	3.424	335.87	3.197	378.92	3.979	370.50	12.213
422.44	4.603	414.08	4.551	Series III		341.55	3.241	379.96	3.935	371.35	15.038
430.50	4.579	418.22	4.584	304.34	3.024	347.21	3.265	381.00	3.997	371.93	17.832
439.54	3.885	422.21	5.883	314.05	3.098	352.84	3.322	Series VI		372.44	18.810
449.02	3.887	425.86	5.486	Series IV		357.05	3.330	366.14	8.254	373.11	17.257
458.52	3.907	429.86	4.417	733.45	3.341	359.85	3.406	366.92	4.877	374.37	4.744
468.06	3.898	434.40	3.982	744.09	3.340	361.80	3.400	367.78	5.205	Series VIII	
477.67	3.884	439.12	3.881	754.81	3.335	362.91	3.525	368.59	6.059	367.37	7.576
487.35	3.842	443.86	3.882	765.57	3.340	364.00	3.602	369.30	7.473	368.02	8.306
497.10	3.813	448.61	3.893	776.39	3.342	365.02	4.542	369.92	8.471	368.64	8.831
506.92	3.807	453.35	3.927	787.27	3.353	365.75	11.035	370.48	9.992	369.22	9.660
516.80	3.790	458.09	3.916	798.19	3.359	366.07	42.986	370.96	11.408	369.76	10.584
526.74	3.786	462.85	3.907	809.16	3.358	366.17	119.64	371.42	11.540	370.26	12.857
536.74	3.787	467.63	3.880	820.17	3.379	366.23	111.93	371.83	13.492	370.66	14.373
546.79	3.783	472.42	3.862	831.19	3.400	366.29	132.12	372.22	13.075	371.08	13.002
556.89	3.790	477.23	3.864	842.24	3.326	366.37	57.647	372.59	14.388	371.52	14.421
567.03	3.795	482.06	3.857	853.31	3.316	366.62	14.875	372.92	17.281	371.92	15.636
577.24	3.756	486.91	3.836	864.40	3.326	367.10	9.390	373.26	13.376	372.29	16.598
Series II		491.78	3.826	875.52	3.321	367.69	8.257	373.63	7.689	372.65	17.536
337.46	3.220	496.66	3.832	886.78	3.332	368.30	8.470	374.14	7.494	373.01	16.622
342.46	3.336	501.56	3.839	898.07	3.334	368.89	8.954	374.95	4.396	373.45	11.007
347.44	3.316	506.48	3.821	909.31	3.318	369.45	9.208	375.99	3.720	374.18	4.503
352.43	3.324	545.15	3.768	920.59	3.352	369.98	10.127	377.06	3.804	375.20	3.842
357.38	3.404	555.25	3.772	931.94	3.277	370.47	11.041	378.13	3.990	376.27	3.789
361.79	5.089	565.41	3.781	943.43	3.328	370.93	11.566			377.35	3.933

TABLE 4—*continued*

T K	$C_{p,m}$ R	T K	$C_{p,m}$ R	T K	$C_{p,m}$ R	T K	$C_{p,m}$ R	T K	$C_{p,m}$ R	T K	$C_{p,m}$ R
$M\{(1/2.995)Cu_{1.995}S\} = 53.035\ g \cdot mol^{-1}$											
High-temperature measurements — University of Oslo											
Series I		618.64	3.798	587.36	3.779	341.47	3.286	395.18	3.998	374.64	17.881
302.14	3.087	628.82	3.834	597.45	3.792	346.40	3.314	399.65	3.976	375.30	24.402
312.35	3.130	639.01	3.839	607.58	3.779	351.31	3.339	403.93	3.973	375.81	32.317
322.50	3.178	649.19	3.911	617.79	3.744	356.19	3.387	Series VI		376.20	40.524
332.57	3.222	659.33	3.956	628.04	3.808	361.01	3.460	298.29	3.026	376.53	46.846
342.57	3.277	669.38	4.104	638.28	3.826	364.91	7.237	305.39	3.102	376.83	43.328
352.50	3.335	679.32	4.205	648.51	3.881	368.24	5.509	312.41	3.126	377.36	17.915
361.75	4.248	689.27	4.129	658.70	3.954	371.48	7.860	319.39	3.150	378.99	4.278
368.96	7.666	699.45	3.946	668.82	4.054	373.81	13.927	326.36	3.175	Series VIII	
373.53	15.455	Series III		678.78	4.213	375.26	25.468	333.30	3.204	418.72	4.183
376.18	28.825	451.56	3.899	688.65	4.266	376.13	42.844	340.22	3.238	420.89	4.667
380.60	6.064	460.91	3.902	698.62	4.133	376.72	56.916	347.11	3.275	422.92	4.523
388.57	3.985	470.29	3.908	709.05	3.648	378.21	9.505	353.97	3.321	425.13	4.030
397.61	3.975	479.72	3.881	720.05	3.394	379.48	5.822	360.75	3.433	427.45	4.089
406.67	3.980	489.22	3.873	732.02	3.359	381.76	4.017	364.85	4.431	429.76	4.397
415.74	4.035	498.78	3.858	743.48	3.347	386.22	3.998	365.90	11.657	432.27	4.374
424.64	4.312	508.41	3.834	754.99	3.330	390.70	3.993	366.75	7.139	434.84	4.226
433.44	4.238	518.09	3.834	766.55	3.348	395.18	3.998	367.91	5.231	437.36	4.069
442.51	3.937	527.83	3.807	Series IV		399.65	3.976	369.19	5.374	439.94	3.902
451.85	3.898	537.62	3.808	303.75	3.128	Series V		370.38	6.145	446.11	3.884
461.28	3.880	547.46	3.807	313.90	3.152	381.76	4.017	Series VII		455.96	3.868
Series II		557.35	3.781	323.99	3.194	386.22	3.998	372.39	8.492	465.68	3.888
598.29	3.768	567.30	3.790	334.01	3.246	390.70	3.993	373.24	10.865	475.43	3.886
608.45	3.774	577.30	3.762					373.94	13.424	485.26	3.862

inputs. In many cases the transitional enthalpy varies from one measurement series to the next, which reflects the varying degree of conversion of the high-temperature phases to the stable assembly during the previous cooling process. In such cases the highest transitional value is most often used in the evaluation of the thermodynamic function values. The thermal history of the samples is summarized in table 6.

For $Cu_{1.90}S$ the reference heat capacity for the anilite to low-digenite transition is estimated from the heat capacities in the pre- and post-transitional regions, compare figure 2. The separation is aided also by the absence of anilite in some of the measurement series due to incomplete low-temperature equilibration. It appears that cooling below 260 K is essential for converting digenite to anilite, compare Series IV, VIII, IX, and XII is contrast to Series V and VI. The maximum value of $\Delta_{trs}H_m = 8.57 \cdot R \cdot K$ represents only about 35 per cent of the value expected for a two-phase mixture of $Cu_{1.75}S$,[3] and djurleite with composition $Cu_{1.934}S$, as claimed by Potter.[11] If our highest result for $Cu_{1.90}S$ represents complete equilibration, the composition of the neighboring phase should be $Cu_{1.915}S$, compare figure 3. Our earlier results for $Cu_{1.80}S$ and $Cu_{1.85}S$ also support this contention, but it should be remarked that the transition temperature is 309.9 K for $Cu_{1.85}S$, and 305.5 K for $Cu_{1.90}S$. The lowering indicates that the peritectoid decomposition of the low-digenite phase occurs below 310 K under equilibrium conditions, but how far is still not known.

TABLE 5. Enthalpy and entropy increments for Cu_xS phases. $R = 8.3144\ J \cdot K^{-1} \cdot mol^{-1}$

Series	Detn.	$\frac{\Delta_{T_1}^{T_2}H_m}{R \cdot K}$	$\frac{\Delta_{T_1}^{T_2}S_m}{R}$	Series	Detn.	$\frac{\Delta_{T_1}^{T_2}H_m}{R \cdot K}$	$\frac{\Delta_{T_1}^{T_2}S_m}{R}$
			$M\{(1/2.90)Cu_{1.90}S\} = 52.691\ g \cdot mol^{-1}$				
(Anilite + djurleite) to low-digenite transition (290 K to 320 K)							
IV	21 to 26	7.18	0.0235	VIII	1 and 2	8.57	0.0280
V	2	1.39	0.0046	IX	2	7.62	0.0250
VI	2	3.15	0.0103	XII	4 to 9	5.16	0.0169
Low-digenite to high-digenite transition (356 K), djurleite- to high-chalcocite transition (363 K to 370 K), and changing composition of high-digenite and djurleite (320 K to 370 K)							
I	4 to 9	65.03	0.1784	XII	19 to 32	88.58	0.2425
II	1 to 14	55.69	0.1523	XIII	1 to 4	86.16	0.2363
			$M\{(1/2.95)Cu_{1.95}S\} = 52.875\ g \cdot mol^{-1}$				
Low-temperature transition (214 K to 228 K)							
IV	2 to 4	2.81	0.0126	XIII	3 to 16	3.22	0.0145
VIII	2 to 4	7.34	0.0331	XIV	3 to 17	2.62	0.0118
XI	3 to 15	6.39	0.0288	XV	1 to 8	4.21	0.0190
XII	1 to 7	4.26	0.0192				
Djurleite to (high digenite + high-chalcocite) transition (350 K to 370 K)							
I	3 to 6	60.76	0.1669	XIX	6 to 10	91.36	0.2511
II	4 to 7	59.66	0.1638	XX	1 to 11	69.76	0.1922
III	2 to 7	54.84	0.1507	XXI	3 to 24	81.19	0.2235
Total increments (350 K to 440 K)							
I		465.7	1.1944	XIX[a]		480.3	1.2547
II		462.9	1.1870	XXI		476.0	1.2258
III		466.7	1.1941	Mean values		470.3	1.2112
[a] Extrapolated above 414 K.							
			$M\{(1/2.98)Cu_{1.98}S\} = 52.982\ g \cdot mol^{-1}$				
(Djurleite + low chalcocite) to high-chalcocite transition (360 K to 367.5 K)							
II	7 to 9	51.46	0.1406	VI	1 and 2	42.47	0.1160
V	13 to 26	44.05	0.1203	VII	1 to 7	50.27	0.1373
Uptake of low chalcocite in high chalcocite (367.5 K to 375 K)							
II	9 to 12	57.85	0.1559	VII	7 to 15	57.71	0.1553
V	26 to 42	58.39	0.1573	VIII	1 to 16	53.98	0.1455
VI	3 to 17	42.47	0.1144				
			$M\{(1/2.995)Cu_{1.995}S\} = 53.035\ g \cdot mol^{-1}$				
(Djurleite + low chalcocite) to high-chalcocite transition (360 K to 367.5 K)							
I	7 and 8	12.45	0.03412	VI	10 to 14	11.31	0.03102
IV	9 to 11	13.07	0.03578				
Uptake of low chalcocite in high chalcocite (367.5 K to 375 K) and of copper in high chalcocite (375 K to 380 K)							
I	8 to 11	118.6	0.3166	VIII	1 to 11	116.9	0.3115
IV	11 to 18	124.7	0.3323				

TABLE 6. Thermal history

Series	Previous treatment	Series	Previous treatment
$Cu_{1.90}S$			
I:	tempered 7 d at 670 K; cooled with furnace	VII:	enthalpy determ., cooled from 332 to 82 K (4 h)
II:	after explor. determ. to 440 K, then from amb. T to 385 K and from amb. T to 365 K	VIII:	cooled to liq. N_2 (4 m)
		IX:	cooled to 200 K overnight, heated to 265 K (8 h)
III:	after 8 a at amb. T cooled to 75 K (44 h)	X:	cooled to 8.7 K (3 d)
IV:	after explor. determ. to 290 K	XI:	cooled to 9.5 K
V:	cooled to 261 K (8 h)	XII:	after 2 m at amb. T
VI:	cooled to 261 K (12 h)	XIII:	after 7 m at amb. T
$Cu_{1.95}S$			
I:	temp. 21 d at 670 K, cooled with furnace	XIII:	up to 283 K, cooled to 184 K (4 h), held at 200 K to 220 K
II:	after explor. determ. to 825 K, and afterwards in the range 500 K to 570 K	XIV:	cooled to 190 K (15 h), down to 135 K (6 h later), heated to 184 K (4 h)
III:	held at 340 K (24 h)	XV:	cooled to 100 K (12 h), heated to 210 K (3 h)
IV:	heated to 750 K after 240 d at amb. T	XVI:	cooled to 51 K (24 h)
V:	cooled to 200 K after 5 a at amb. T	XVII:	cooled to 4.1 K (5 d)
VI:	Cooled from 245 K to 200 K overnight	XVIII:	heated to 90 K, enthalpy determ.
VII:	cooled to 84 K (11 h)	XIX:	after 70 d at amb. T
VIII:	cooled from 210 K to 200 K	XX:	held at 340 (2 d)
IX:	cooled to 113 K	XXI:	after explor. determ. to 450 K and 14 d at 358 K
X:	after two enthalpy determ., 180 K to 300 K		
XI:	cooled to 147 K overnight		
XII:	cooled to 52 K (59 h), heated to 200 K		
$Cu_{1.98}S$			
I:	tempered at 670 K (20 d), cooled with furnace	V:	after determ. to 1000 K and 5 a at amb. T
II:	heated to 330 K	VI:	after explor. determ. to 386 K
III:	after 150 d at amb. T	VII:	after 1 a at amb. T
IV:	heated to 725 K (20 h)	VIII:	after 3 d at 365 K
$Cu_{1.995}S$			
I:	tempered at 670 K (20 d), cooled with furnace	V:	cooled to 375 K (12 h)
		VI:	after 12 a at amb. T
II:	heated at 590 K (17 h)	VII:	held at 370 K (24 h)
III:	heated to 440 K after 3 d at amb. T	VIII:	heated to 415 K (42 h)
IV:	after 2 d at amb. T		

The transitions of low digenite to high digenite, and of djurleite to (high digenite + high chalcocite), both occur in the region 350 K to 370 K. In addition, the digenite phase changes composition from about $Cu_{1.77}S$ to $Cu_{1.83}S$ on heating from 300 K to 370 K. Furthermore, the djurleite phase might also vary in composition. The combined effects result in a maximum transitional value for Series XII. The low- to high-digenite transition appears as a slight maximum around 356 K in Series II and around 351 K in Series XII, while the maximum is at 352.6 K in $Cu_{1.75}S$, at 355.3 K in $Cu_{1.80}S$, and is observable as a bulge around 355 K in the low- to high-digenite transition in $Cu_{1.85}S$. The transition of djurleite to (high digenite + high chalcocite)

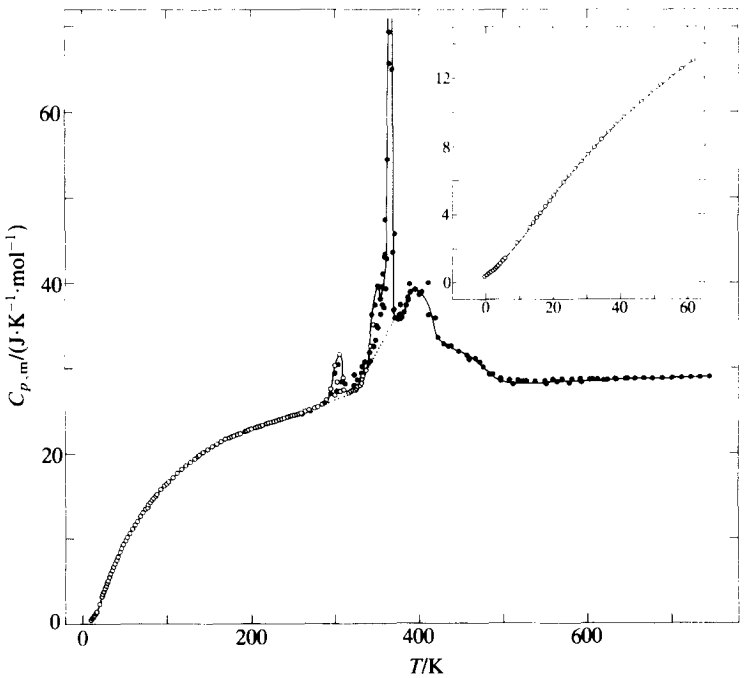

FIGURE 2. Molar heat capacity of (1/2.90)$Cu_{1.90}S$. ○, U. of M.; ●, U. of O.; ···, reference values in transition regions.

shows up as a substantial maximum over a 4 K interval around 366 K, compare Series XII.

The enthalpy of the transitions is evaluated by subtracting $C_{p,m}/R = -3.1620 + 0.020086(T/K)$ over the range 320 K to 370 K. The results for the more thoroughly equilibrated sample, compare tables 5 and 6, are considerably higher than those obtained after comparatively short resting times at ambient temperatures and below. Thus, the mean values from Series XII and XIII are chosen.

The high heat capacity persists above 370 K for $Cu_{1.90}S$ and returns to normal at about 500 K. We ascribe it primarily to the changing composition of the high-digenite phase from $Cu_{1.83}S$ to $Cu_{1.90}S$ by uptake of high chalcocite. The maximum around 400 K presumably reflects the most rapid change in composition of high digenite with temperature. Changes in the phase composition of high chalcocite constitutes another possible contribution, which then ought to be more prominent in $Cu_{1.95}S$.

The heat capacity of $Cu_{1.95}S$ is shown in figure 4. A small transition is observed around 220 K. The background level for the transition is interpolated by polynomial fitting of the heat capacities in the pre- and post-transitional regions. Again, the transitional enthalpy varies as result of previous cooling procedures, compare tables 5 and 6. The highest value, $\Delta_{trs}H_m = 7.34 \cdot R \cdot K$, is obtained in Series VIII, *i.e.* after cooling to 84 K (11 h), measurements up to 210 K (Series VII), and cooling to

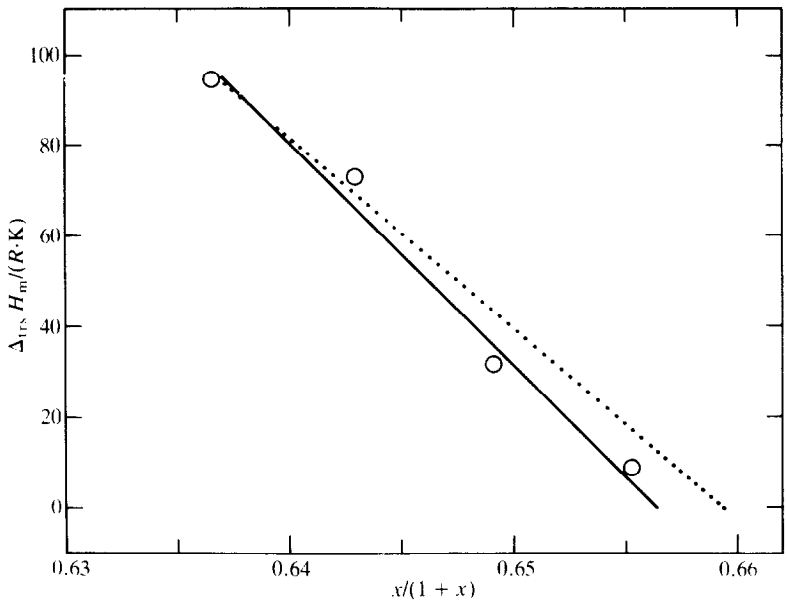

FIGURE 3. Enthalpy of decomposition of anilite as function of mole fraction of Cu in Cu_xS with x = 1.90, 1.85, 1.80, and 1.75; ···, expected values with djurleite composition equal to $Cu_{1.938}S$.

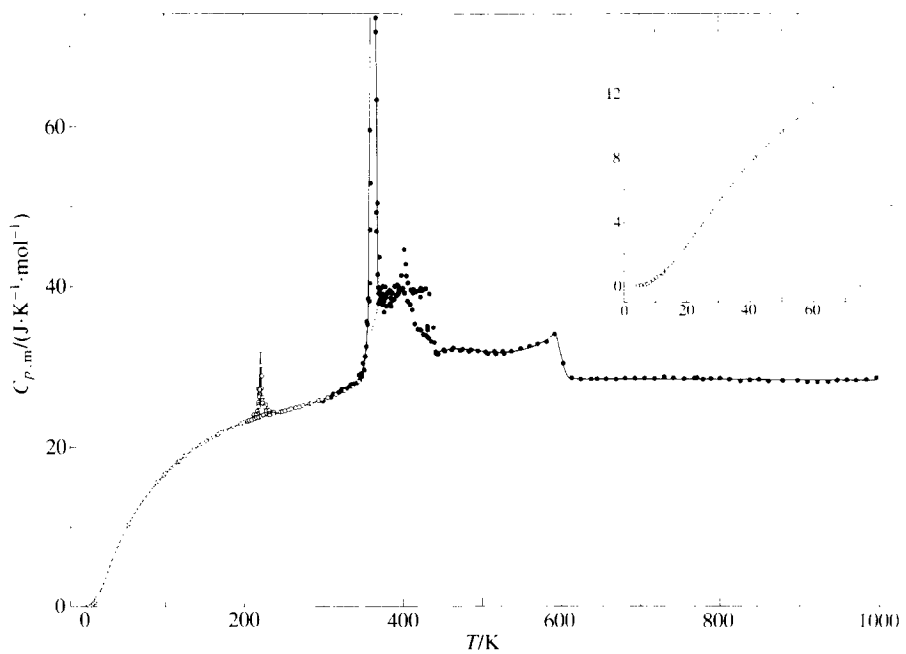

FIGURE 4. Molar heat capacity of $(1/2.95)Cu_{1.95}S$. ○, U. of M.; ●, U. of O.; ···, reference values in transition regions.

200 K before the start. In the absence of contradictory evidence this value is for the present taken as representing complete conversion of the low-temperature phase to the tetragonal phase in the sample. The amounts of the low-temperature and tetragonal phases vary depending upon the heat treatment and constitute fractions which are not known with certainty. The transition is seen to be absent in Series V and VI, indicating that cooling to 200 K is not in itself sufficient to obtain conversion to the low-temperature phase.

The djurleite to (high-digenite + high-chalcocite) transition presents itself as a broad heat-capacity maximum in the range 361 K to 367 K, compare Series XXI. The background level for the transition is represented by $C_{p,\mathrm{m}}/R = -14.577 + 0.051750(T/\mathrm{K})$ over the range 350 K to 370 K. The enthalpy of the djurleite transition is highest in Series XIX, but it is seen that tempering at 358 K for 14 d (Series XXI) is also rather effective in equilibrating the sample. As a consequence of such equilibration, the enthalpy increment in the range 370 K to 440 K is lower for Series XXI than for the other series. For Series XIX similarly, a high enthalpy increment in the range 350 K to 370 K is followed by a low increment in the range 370 K to 415 K.

In the evaluation of the thermodynamic properties of $Cu_{1.95}S$ the mean results of all five Series have been used for obtaining the total increments over the region 350 K to 440 K. Since Series XIX probably represents the best equilibrated sample, it has been used for obtaining the 350 K to 370 K increments. Furthermore, the 222 K transition increments have not been included, as they presumably are caused by the presence of metastable phases. The high heat capacity in the range 367 K to 430 K is due to the exsolution of high digenite from high chalcocite, whereas the smaller excess heat capacity persisting up to 610 K is due to the increasing solubility of almost stoichiometric high chalcocite in high digenite.

The transitional evaluations for $Cu_{1.98}S$ are complicated by the partial overlap of the djurleite to low-chalcocite transition with that of low chalcocite to high chalcocite. The present heat-capacity results for $Cu_{1.98}S$, compare table 4 Series V and also figure 5, give no indications of the 363 K transition reported by Potter,[11] but a marked confirmation of the 366 K transition.

A heat-capacity maximum of $100 \cdot R$ is observed in the range 366.1 K to 366.3 K, compare Series V and VII, which we ascribe to the eutectoid formation of high chalcocite from (djurleite + low chalcocite). Evaluations with background level $C_{p,\mathrm{m}}/R = -5.3851 + 0.024467(T/\mathrm{K})$ from 360 K to 375 K give close to the same values for Series II and VII over the range 360 K to 367.5 K. The mean value $\Delta_{\mathrm{trs}}H_{\mathrm{m}} = 50.87 \cdot R \cdot \mathrm{K}$ is chosen. For the solution of low chalcocite in high chalcocite from 367.5 K to 375 K the mean value of Series II, V, VII, and VIII is $\Delta_{\mathrm{trs}}H_{\mathrm{m}} = 56.98 \cdot R \cdot \mathrm{K}$. Series VI obviously does not pertain to a well equilibrated sample. The high heat capacity of $Cu_{1.98}S$ above 366.2 K indicates that it is still not single-phase material. The solution process occurs over a range of about 4 K with heat capacities ranging only between $10 \cdot R$ and $24 \cdot R$, compare Series I, II, V, VI, and VIII. Hence chalcocite is probably homogeneous close to the composition $Cu_{1.97}S$ when formed at 366.2 K, and changes its composition towards $Cu_{1.98}S$ by uptake of low chalcocite. This process appears to be largely completed at 374 K.

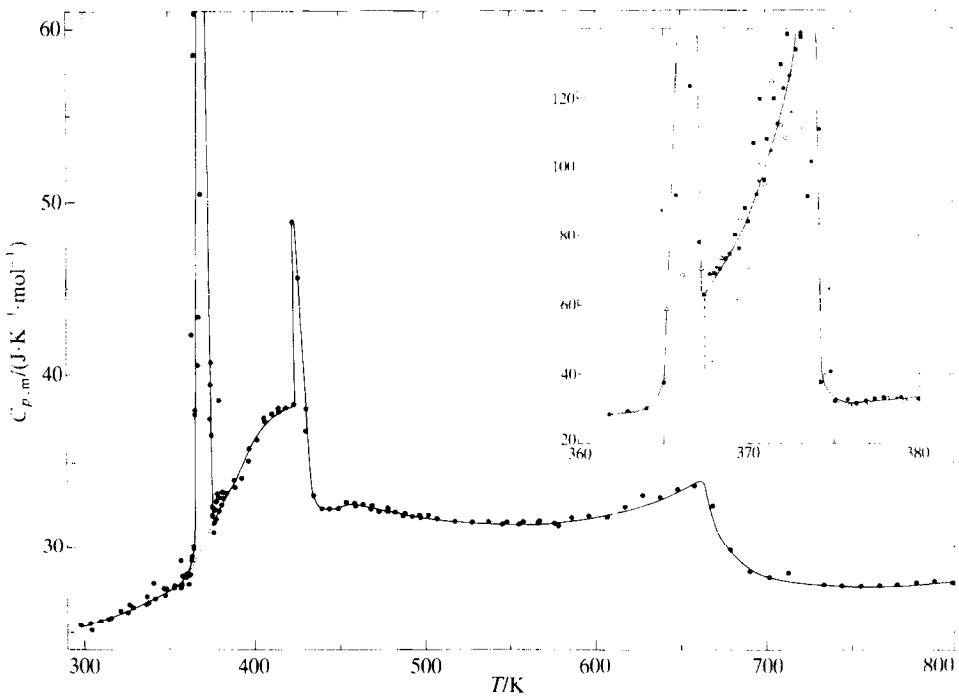

FIGURE 5. Molar heat capacity of (1/2.98)$Cu_{1.98}S$. Details in insert: ···, reference values in transition regions; – – –, dividing line, 367.5 K; +, Series II; ●, Series V; ○, Series VI; △, Series VII; ■, Series VIII.

In addition to this solution process, a further process terminates around 430 K and another around 670 K. The former begins at about 390 K and is ascribed to the exsolution of high digenite from high chalcocite, which thus becomes more closely stoichiometric. The peak near 430 K is presumably due to a rapid conclusion of the exsolution process due to overheating. Superimposed on the decreasing heat capacity of high chalcocite with temperature comes the reaction component for solution of high chalcocite in high digenite, which is complete at 670 K. The steady decrease in the range 470 K to 530 K is indicative of the presence of relatively large amounts of high chalcocite in $Cu_{1.98}S$.

The heat capacity of $Cu_{1.995}S$ is shown in figure 6. Just as for $Cu_{1.98}S$, a rather sharp maximum is observed near 366 K, followed by a broader one peaking at 376.7 K. Again, the former peak is attributed to the eutectoid formation of high chalcocite from (low chalcocite + djurleite), while the latter is related to the uptake of low chalcocite in high chalcocite. Remarkably, the heat capacity remains higher for $Cu_{1.995}S$ than for $Cu_{2.00}S$ in a narrow range above 377 K, which indicates that high chalcocite contains slightly more sulfur than does low chalcocite in this temperature range.

The enthalpy of the transitions is evaluated after subtracting a background level represented by $C_{p,m}/R = -7.334 + 0.02990(T/K)$ in the range 360 K to 380 K. The

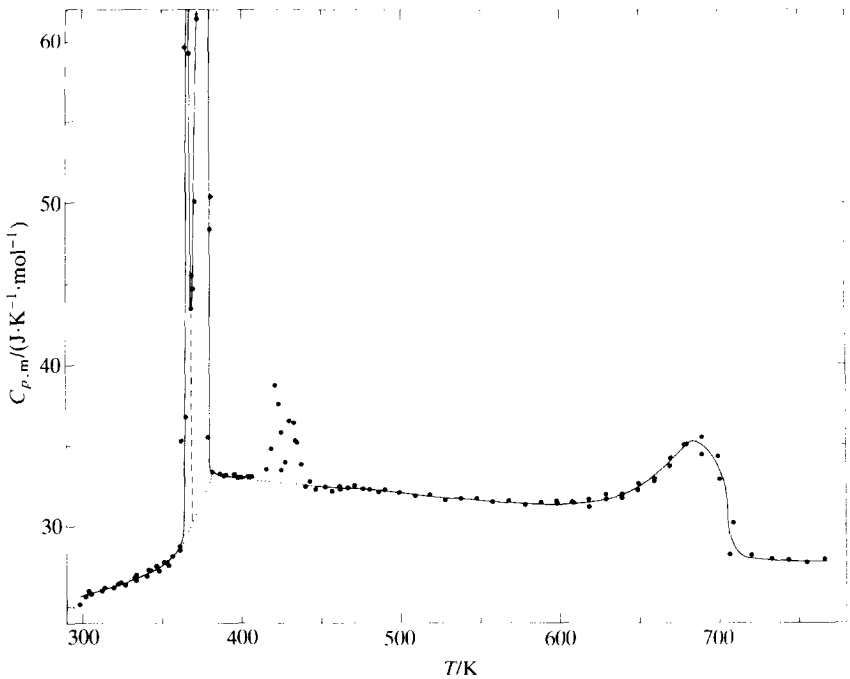

FIGURE 6. Molar heat capacity of (1/2.995)$Cu_{1.995}S$. ····, Reference lines in transitional regions; — — —, dividing line, 367.5 K.

enthalpy effects of the two transitions are presently divided at 367.5 K so that the eutectoid formation resides in the lower peak. Over the range 360 K to 367.5 K the mean value of the transitional enthalpy is $\Delta_{trs}H_m = 12.28 \cdot R \cdot K$, and over the range 367.5 K to 380 K it is $120.0 \cdot R \cdot K$. The large unit cell of low chalcocite ($Cu_{96}S_{48}$) implies high structural order and thus a very narrow homogeneity range.

In the range 380 K to 420 K and also above 440 K the heat capacity of $Cu_{1.995}S$ is very reproducible and slightly decreasing. The high values in the intermediate range are presumably due to the rapidly changing sulfur-rich composition limit of high chalcocite towards stoichiometry with increasing temperature. The excess enthalpy above a smoothly decreasing heat capacity in the region 410 K to 440 K amounts to $8.3 \cdot R \cdot K$, which for the present will be included in the thermodynamic functions for $Cu_{1.995}S$. At about 620 K the heat capacity departs from its steadily decreasing path and rises to a maximum of about $4.3 \cdot R$ around 790 K. The associated solution of high chalcocite in high digenite is complete around 710 K, where the heat capacity regains its normal course.

PHASE RELATIONS IN THE $Cu_{1.90}S$ TO $Cu_{2.00}S$ REGION

According to Potter's[11] phase diagram for the $Cu_{2-x}S$ region (compare figure 7) a sample with composition $Cu_{1.995}S$ should consist of a mixture of (low chalcocite +

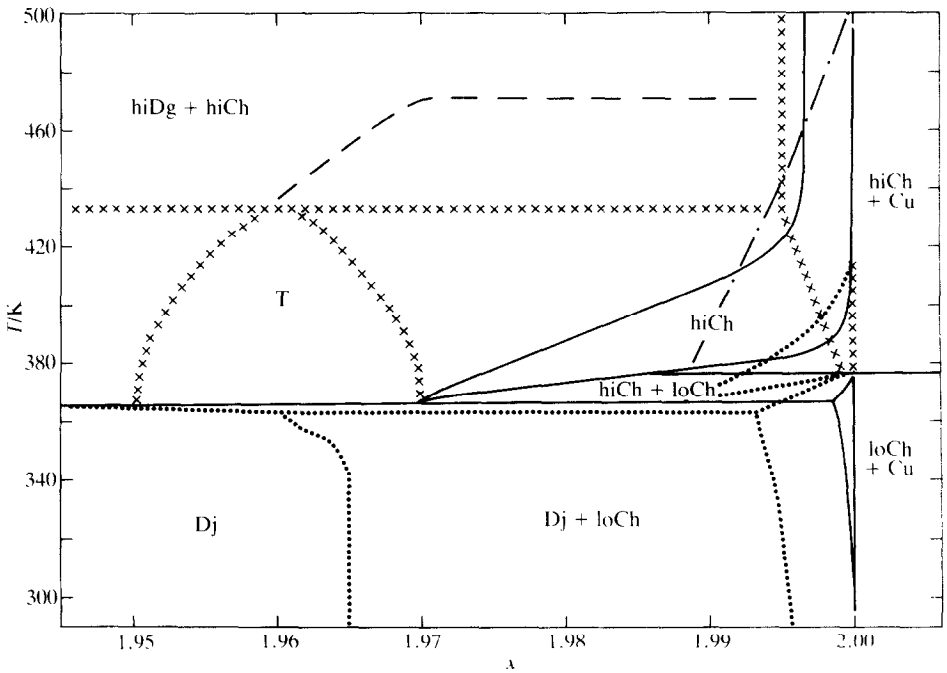

FIGURE 7. Phase relations in the low-chalcocite high-chalcocite region according to different authors: ●, Potter;[11] × ×, Kubaschewski;[21] – –, Dumon *et al.*[26] (high digenite + tetragonal phase + high-chalcocite) between 375 K and the line from $Cu_{1.96}S$ to $Cu_{1.99}S$; – · –, Dumon *et al.*[26] high chalcocite to the right of this line.

djurleite) at ambient temperature and become single-phase low chalcocite around 320 K. It should remain so up to 365 K, at which temperature the eutectoid transformation to high chalcocite should start. The biphasic reaction terminates at 370 K and the high chalcocite remains homogeneous up to 380 K. Above this temperature high digenite is exsolved until the high chalcocite becomes practically stoichiometric, *i.e.* $Cu_{>1.999}S$, at 420 K. Thus, the low- to high-chalcocite enthalpy increment should develop in the 365 K to 370 K interval, while normal high-chalcocite heat capacity ($\approx 4 \cdot R$) should show up in the range 370 K to 380 K. The compositional change of high chalcocite ($dx/dT = 0.00002 \cdot K^{-1}$ at 380 K) is expected to raise the heat capacity by about $0.2 \cdot R$ above the $C_{p,m}$(lattice) value in the beginning and to decay to zero at about 420 K. The present results for $Cu_{1.995}S$ do not correspond well with the above picture. A practically isothermal enthalpy acquisition occurs at 366.2 K, followed by a small phase-reaction contribution in the 367 K to 371 K region. The contribution rises markedly with further increase in temperature and reaches $56.89 \cdot R$ over the interval 376.46 K to 376.98 K. Above 380 K normal high-chalcocite heat capacity obtains. Also for $Cu_{1.98}S$ we find an isothermal enthalpy absorption at 366.2 K, with about four times the magnitude of that for $Cu_{1.995}S$. In $Cu_{1.95}S$ the effect is absent, or overshadowed by the decomposition reaction of djurleite to high digenite and low chalcocite in the 360 K

to 365 K region (compare Series XXI). At present we do not have enough experimental values to locate the high-chalcocite eutectoid composition exactly, but indications are that it is close to the composition $Cu_{1.97}S$. The low- to high-chalcocite transition is practically complete at 374 K. Accordingly, the decay of the eutectoid reaction at 366.2 K with increasing copper content, and also the fact that it is only about 10 per cent of the total reaction enthalpy in the range 360 K to 375 K for $Cu_{1.995}S$, substantiate the copper-rich composition limit of low chalcocite as not below $Cu_{1.9995}S$ at 366.2 K. Since, on the other hand, the eutectoid reaction for $Cu_{1.98}S$ is only one half of the total, the composition of the high-chalcocite eutectoid ought to be around $Cu_{1.97}S$ (with an uncertainty dependent upon the enthalpy increment for compositional change of the high-chalcocite phase).

The presently proposed phase diagram for the region $Cu_{1.96}S$ to Cu_2S differs substantially from earlier versions, see figure 7. The complex phase diagram proposed by Dumon *et al.*[26] was based on anomalies in the e.m.f. of the cell $Cu|CuBr|Cu_{2-x}S|C$ with temperature. The homogeneity range of high chalcocite was found to decrease with increasing temperature above 377 K in agreement with the present findings. No evidence is found here which supports their reported increase in the solubility of high digenite in high chalcocite at even higher temperatures. Dumon *et al.*[27] found that the high-chalcocite phase becomes stoichiometric at 500 K and that the solubility of high digenite in high chalcocite increases rapidly up to 590 K, with a limiting composition $Cu_{1.97}S$ for high chalcocite. We do not see the consequential decay in solution reaction heat capacity either in the region 520 K to 690 K for $Cu_{1.995}S$ or in the region 570 K to 640 K for $Cu_{1.98}S$. Furthermore, the homogeneity range found here for low chalcocite is much narrower than reported by Dumon *et al.*[26] and Potter.[11] Potter also reported a broad homogeneity range for the djurleite phase.[11] Taking the large unit cell of the compound, which implies high structural order, into consideration, it is tempting to suggest the existence of two distinct phases with closely related structures. The phase diagram proposal by Kubaschewski[21] differs from the present one and that by Dumon *et al.*[26] in that the homogeneity range of high chalcocite is taken to increase with increasing temperature. Furthermore, the heat-capacity effects around, 430 K ascribed to disappearance of the tetragonal phase (T) by Kubaschewski,[21] is interpreted here as arising from the compositional change of high chalcocite. The tetragonal phase and its low-temperature polymorph may in our opinion be metastable phases originating in the cooling process of high chalcocite with approximate composition $Cu_{1.97}S$.

THERMODYNAMIC PROPERTIES

The experimental heat capacities for the low- and high-temperature series were fitted to polynomials by the method of least squares. The fitting and especially the joins between the fitted segments were checked by inspection of plots of $dC_{p,m}/dT$ against T. The polynomials were then integrated by Simpson's rule, to yield values of thermodynamic functions at selected temperatures presented in table 7. Within the transition regions the heat-capacity values were read from large-scale plots and the thermodynamic functions were calculated by integration of the curves. At the lowest

TABLE 7. Thermodynamic properties ($R = 8.3144\ J \cdot K^{-1} \cdot mol^{-1}$)

T / K	$C_{p,m}/R$	$\Delta_0^T S_m^\circ/R$	$\Delta_0^T H_m^\circ/R \cdot K$	Φ_m°/R	T / K	$C_{p,m}/R$	$\Delta_0^T S_m^\circ/R$	$\Delta_0^T H_m^\circ/R \cdot K$	Φ_m°/R
				$M\{(1/2.90)Cu_{1.90}S\} = 52.691\ g \cdot mol^{-1}$					
0	0	0	0	0	260	2.984	4.234	520.69	2.2314
10	0.0496	0.0162	0.1226	0.0039	280	3.081	4.458	581.12	2.3824
15	0.1544	0.0542	0.6085	0.0136	290	3.136	4.567	612.23	2.4559
20	0.2983	0.1179	1.731	0.0314	298.15	(3.166)	4.654	637.91	2.5148
25	0.4543	0.2011	3.610	0.0567	300	(3.170)	4.674	543.77	2.5280
30	0.6112	0.2978	6.275	0.0886	305	(3.185)	4.727	659.66	2.5637
40	0.9009	0.5144	13.875	0.1675	305	(3.185)	4.755	668.22	2.5637
50	1.146	0.7433	24.141	0.2605	320	3.265	4.909	716.43	2.6702
60	1.356	0.9705	36.678	0.3592	340	3.933	5.223	839.62	2.7537
70	1.541	1.1937	51.181	0.4625	370	4.270	5.694	991.86	3.0129
80	1.705	1.410	67.425	0.5675	430	3.932	6.366	1260.1	3.4353
90	1.852	1.620	85.238	0.6729	440	3.904	6.456	1299.3	3.5031
100	1.983	1.822	104.42	0.7778	450	3.832	6.543	1338.1	3.5689
120	2.207	2.205	146.40	0.9850	500	3.455	6.924	1519.1	3.8861
140	2.397	2.559	192.49	1.1841	550	3.409	7.250	1689.7	4.1773
160	2.549	2.890	242.03	1.3773	600	3.443	7.548	1861.1	4.4460
180	2.659	3.197	294.15	1.5628	650	3.451	7.824	2033.5	4.6952
200	2.753	3.482	348.28	1.7406	700	3.478	8.080	2206.7	4.9280
220	2.841	3.844	404.23	2.0066	750	3.477	8.321	2380.6	5.1469
240	2.911	3.998	461.77	2.0740					
				$M\{(1/2.95)Cu_{1.95}S\} = 52.875\ g \cdot mol^{-1}$					
0	0	0	0	0	260	2.978	4.262	523.04	2.2503
5	0.0048	0.0020	0.0077	0.0005	280	3.044	4.485	583.27	2.4019
10	0.0505	0.0156	0.1188	0.0037	298.15	3.109	4.679	639.13	2.5353
15	0.1582	0.0550	0.6207	0.0136	300	3.115	4.698	644.87	2.5476
20	0.3026	0.1197	1.762	0.0316	320	2.223	4.902	708.04	2.6884
25	0.4615	0.2040	3.669	0.0573	340	3.361	5.101	773.74	2.8244
30	0.6194	0.3023	6.374	0.0898	350	3.536	5.200	808.10	2.8909
40	0.9099	0.5211	14.053	0.1698	370	4.570	5.676	980.44	3.0260
50	1.160	0.7517	24.435	0.2631	440	3.969	6.411	1278.4	3.5056
60	1.372	0.9825	37.122	0.3638	450	3.897	6.497	1316.7	3.5711
70	1.556	1.208	51.782	0.4634	500	3.816	6.903	1509.2	3.8844
80	1.718	1.427	68.171	0.5746	550	3.874	7.268	1700.7	4.1756
90	1.863	1.638	86.079	0.6816	600	3.845	7.611	1898.2	4.4476
100	1.995	1.841	105.38	0.7872	650	3.380	7.892	2073.1	4.7021
120	2.223	2.225	147.64	0.9947	700	3.446	8.145	2243.8	4.9391
140	2.405	2.582	193.98	1.1965	750	3.433	8.382	2416.1	5.1608
160	2.553	2.914	243.63	1.3913	800	3.405	8.603	2586.9	5.3691
180	2.672	3.222	295.93	1.5779	850	3.403	8.809	2757.1	5.5654
200	2.767	3.508	350.36	1.7562	900	3.389	9.003	2927.0	5.7511
220	2.846	3.775	406.51	1.9272	950	3.384	9.187	3096.2	5.9271
240	2.913	4.027	464.12	2.0932	1000	3.420	9.361	3266.5	6.0945

T / K	$C_{p,m}/R$	$\Delta_{298.15K}^T S_m^\circ/R$	$\Delta_{298.15K}^T H_m^\circ/R \cdot K$	T / K	$C_{p,m}/R$	$\Delta_{298.15K}^T S_m^\circ/R$	$\Delta_{298.15K}^T H_m/R \cdot K$
			$M(1/2.98)Cu_{1.98}S = 52.982\ g \cdot mol^{-1}$				
298.15	3.042	0	0	600	3.827	2.938	1260.4
300	3.051	0.019	5.63	650	4.025	3.252	1456.6
320	3.123	0.218	67.25	700	3.395	3.529	1643.4

TABLE 7—*continued*

T / K	$C_{p,m}/R$	$\Delta_{298.15K}^{T} S_m/R$	$\Delta_{298.15K}^{T} H_m/R \cdot K$	T / K	$C_{p,m}/R$	$\Delta_{298.15K}^{T} S_m/R$	$\Delta_{298.15K}^{T} H_m/R \cdot K$
340	3.253	0.411	131.10	750	3.349	3.760	1810.8
360	3.423	0.600	197.20	800	3.361	3.977	1978.8
380	3.921	1.079	374.27	850	3.334	4.180	2146.2
440	3.915	1.751	648.77	900	3.334	4.371	2312.8
450	3.897	1.839	687.72	950	3.335	4.551	2479.7
500	3.820	2.247	881.26	1000	3.384	4.723	2646.9
550	3.778	2.608	1070.9				
			$M(1/2.995)Cu_{1.995}S = 53.035\ g \cdot mol^{-1}$				
298.15	3.027	0	0	500	3.889	2.257	884.45
300	3.061	0.019	5.63	550	3.789	2.623	1076.2
320	3.158	0.221	68.16	600	3.771	2.950	1264.4
340	3.262	0.415	132.32	650	3.891	3.255	1455.1
360	3.430	0.605	198.81	700	(4.02)	3.564	1660.7
380	4.028	1.161	405.56	750	3.332	3.800	1832.0
430	3.981	1.664	609.42	770	3.344	3.888	1898.5
450	3.895	1.849	690.82				

temperatures the heat capacities were smoothed with the aid of plots of $C_{p,m}/T$ against T^2 and the functions were evaluated by extrapolation of this function. From such plots γ was found to be zero within experimental error limits for both $Cu_{1.90}S$ and $Cu_{1.95}S$ $\{C_{p,m}/R = 4.871 \cdot 10^{-5}(T/K)^3$ and $4.931 \cdot 10^{-5}(T/K)^3$, respectively$\}$.

The portion of this work done at the University of Michigan was supported by the Structural Chemistry and Chemical Thermodynamics Program, Division of Chemistry, National Science Foundation, under Grant No. CHE-7710049, whereas the work done at the University of Oslo was supported by the Norwegian Research Council for Science and the Humanities. The assistance of Bjørn Lyng Nielsen with the preparation of the samples and in the higher-temperature calorimetric measurements is gratefully acknowledged.

REFERENCES

1. Grønvold, F.; Westrum, E. F., Jr. *J. Chem. Thermodynamics* **1987,** 19, 1183.
2. Westrum, E. F., Jr.; Stølen, S.; Grønvold, F. *J. Chem. Thermodynamics* **1987,** 19, 1199.
3. Grønvold, F.; Stølen, S.; Westrum, E. F., Jr.; Galeas, C. G. *J. Chem. Thermodynamics* **1987,** 19, 1305.
4. Djurle, S. *Acta Chem. Scand.* **1958,** 12, 1415.
5. Roseboom, E. H. *Am. Mineral.* **1962,** 47, 1181.
6. Takeda, H.; Donnay, J. D.; Appleman, D. E. *Z. Kristallogr.* **1967,** 125, 414.
7. Cavalotti, P.; Salvago, G. *Electrochemica Metalli* **1969,** 4, 181.
8. Cook, W. R., Jr. *U.S. Natl. Bur. Standards Spec. Publ.* **1972,** 364, 703.
9. Luquet, H.; Gustavino, F.; Bugnot, J.; Vaissière, J. C. *Mater. Res. Bull.* **1972,** 7, 955.
10. Mathieu, H. J.; Rickert, H. *Z. Phys. Chem. NF* **1972,** 79, 315.
11. Potter, R. W. *Econ. Geol.* **1977,** 72, 1524.
12. Evans, H. T., Jr. *Nature* **1971,** 232, 69.
13. Evans, H. T., Jr. *Science* **1979,** 203, 356.
14. Evans, H. T., Jr. *Z. Kristallogr.* **1979,** 150, 299.
15. Janosi, A. *Acta Cryst.* **1964,** 17, 311.

16. Eliseev, E. N.; Rudenko, L. E.; Sinev, L. A.; Koshurnikov, B. K.; Solovov, N. I. *Mineralog. Sb. L'Vovsk. Gos. Univ.* **1964,** 18, 385.
17. Cook, W. R., Jr.; Shiozawa, L.; Augustine, F. *J. Appl. Phys.* **1970,** 41, 3058.
18. Skinner, B. J. *Econ. Geol.* **1970,** 65, 724.
19. Mulder, B. J. *Kristall und Technik* **1973,** 8, 825.
20. Kazinets, M. M.; Ivanova, I. V.; Shafizade, R. B. *Phase Transitions* **1979,** 1, 199.
21. Kubaschewski, P. *Ber. Bunsenges. Phys. Chem.* **1973,** 77, 74.
22. Evans, H. T., Jr. *Nat. Phys. Sci.* **1971,** 232, 69.
23. Potter, R. W.; Evans, H. T., Jr. *J. Res. U.S. Geol. Surv.* **1976,** 4, 205.
24. Westrum, E. F., Jr.; Furukawa, G. T.; McCullough, J. P. *Experimental Thermodynamics, Vol. I.* McCullough, J. P.; Scott, D. W.: Editors. Butterworths: London. **1968,** p. 133.
25. Grønvold, F. *Acta Chem. Scand.* **1967,** 21, 1695.
26. Dumon, A.; Lichanot, A.; Gromb, S. *J. Chim. Phys.* **1974,** 71, 407.